Supplemental Data

Table 1S: Primers for qRT-PCR.

	Accession Number	Forward	Reverse	Species
ATGL	NM_025802.3	TGTGGCCTCATTCCTCCTAC	TCGTGGATGTTGGTGGAGCT	Mouse
ADPN	NM_054088.3	ATTCCCCTCTTCTCTGGCCTA	ATGTCATGCTCACCGTAGAAAGG	Mouse
TGH	NM_053200.2	CTCAGAGACCCACAGAGCCCTTGTC	AAGCTGTGCACGCAGCAAGAGA	Mouse
AADAC	NM_023383.1	TCCCACCCACGTCTGATGAGC	AAGCCCCGCCTGAGAGCCAT	Mouse
CGI58	NM_026179.2	CTTGCTTGGACACAACCTG	GAGGTGACTAACCCTTGATGG	Mouse
Cyclophilin	NM_008907.1	CTTCTTGCTGGTCTTGCCATTCCT	GGATGGCAAGCATGTGGTCTTTG	Mouse
CPT1a	NM_013495.2	TTAACAGCAACTACTACGCC	CCAGAAGACGAATAGGTTTGAG	Mouse
CPT2	NM_009949.1	CAGTTCAGGAAGACAGAAGTG	CGAAGTGTCTTCAGAAACCG	Mouse
LCAD	NM_007381.3	AAACGTCTGGACTCCGGTTC	GTACCACCGTAGATCGGCTG	Mouse
MCAD	NM_007382.4	TCAAGATCGCAATGGGTGCT	GCTCCACTAGCAGCTTTCCA	Mouse
SCAD	NM_007383.2	GTGACCTGCAACCGAGAAGA	AGGGCGGCTCAAATGAAGAA	Mouse
SIRT3	NM_022433.2	CGCTAAACTTCTCCCGGGTT	ACACAGAGGGATATGGGCCT	Mouse
PDK4	NM_013743.2	GCCAACCCTACGGATCCTAAC	TGTTCACTAAGCGGTCAGGC	Mouse
ATGL	NM_020376.3	AAGCGGAGGATTACTCGCAG	AAGCGGATGGTGAAGGACAG	Human
Cyclophilin	NM_021130	AAGACTGAGTGGTTGGATGG	CGAGAGCACAAAGATTCTAGG	Human
CPT1a	NM_001031847.2	AGTTCTCTTGCCCTGAGACG	GTGATGTCCATGGTCTCCTCC	Human
CPT2	NM_000098.2	GTAGCACTGCCGCATTCAAG	GCCATGGTACTTGGAGCACT	Human
LCAD	NM_001608.3	ATACGGTTGCCAGCTAGTGC	TGCACTGTCTGTAGGTGAGC	Human
MCAD	NM_000016.4	GCTGCAGGGTCCTGAGAAGTA	TATTCTGCAGCCACTGGGATG	Human
SCAD	NM_000017.2	GGAACATCTCTTCCCAGCGG	GAGGGCAAAGCAGCCAATTT	Human
SIRT3	NM_001017524.2	TGGCGGCAGGGACGATTATT	ATCGTACTGCTGGAGGTTGC	Human
PDK4	NM_002612.3	TGGTTTTGGTTACGGCTTGC	AGTGTCCCTCTTCACATGGC	Human
MTTP	NM_008642.1	CACAATTATGACCGTTTCTCCA	CAATCACCACCTGACTACCA	Mouse
FGF21	NM_020013.4	TACACAGATGACGACCAAGAC	AAAGTGAGGCGATCCATAGAG	Mouse

LXRα	NM_013839.3	GTTTCTCCTGATTCTGCAACG	ACCCTATCCCTAAAGCAACC	Mouse
PGC1β	NM_133249.2	GTGTTCGGTGAGATTGTAGAG	CAGATGTGGGATCATAGTCAG	Mouse
CYP7α	NM_007824.2	TGGAATAAGGAGAAGGAAAGTAGG	AGGGAGTTTGTGATGAAGTG	Mouse
PPARγ2	NM_011146.3	GAGCACTTCACAAGAAATTACC	TCTACTTTGATCGCACTTTGG	Mouse

Supplementary Figures

FIGURE 1S. *Effect of diet and Elovl5 activity on glycerol-3-phosphate 2-O-acyl transferase 1 (GPAT1) expression in livers of lean and obese mice.* Mouse liver RNA from fasted and refed lean and obese mice infected with either Ad-Luc or Ad-Elovl5 was prepared and assayed for GPAT1 and cyclophilin mRNA by qRT-PCR. GPAT1 mRNA abundance is represented as mRNA Abundance-Fold Change from fasted lean (LFD) Ad-Luc infected mice; mean ± SD, n=6; ***a***, $p<0.05$ versus fasted lean LFD-fed mice infected with Ad-Luc; ***b***, $p<0.05$ versus fasted lean LFD-fed mice infected with Ad-Elovl5; ***c***, $p<0.05$ versus refed lean LFD-fed mice infected with Ad-Luc; one-way ANOVA plus post-hoc HSD.

FIGURE 2S. *Diet and Elovl5 effects on hepatic **microsomal** transfer protein (MTTP) expression.* Mouse liver RNA from fasted lean (LFD) and obese (HFD) mice infected with either Ad-Luc or Ad-Elovl5 was assayed for MTTP and cyclophilin mRNA by qRT-PCR. MTTP mRNA was represented relative to cyclophilin as mean ± SD, n=6.

FIGURE 3S. *Hepatic nuclear abundance of PPAR subtypes in fasted lean and obese mice*. Panels A & B: Hepatic nuclear extracts from fasted lean and obese mice infected with Ad-Luc or Ad-Elovl5 were assayed for PPARα and TATA-binding protein (TBP) [Methods]. Panel A is the representative immunoblot with extracts from 2 separate mice per group. Panel B is the quantified level PPARα relative to the loading control TBP; mean ± S.D., n=4. ***a***, $p<0.05$ versus LFD fed mice infected with Ad-Luc. Panels C & D. The nuclear abundance of PPARα, PPARδ, PPARγ1 and PPARγ2 was quantified as

described above. Livers from obese (HFD-fed) mice infected with Ad-Luc or Ad-Elovl5 were used in this analysis. Panel C is the representative immunoblot with extracts from 3 mice/group. Panel D is the quantified level of the PPAR subtypes. Results are from 2 separate studies and are expressed as mean ± SD, n=6. *a*, $p \leq 0.05$ versus high fat (HF) diet fed Ad-Luc infected mice; one-way ANOVA with post-hoc HSD.

FIGURE 4S. *Fatty acid oxidation of saturated, mono- and polyunsaturated fatty acids in AML12 cells.* AML12 cells were treated with ^{14}C-label fatty acids at 100 μM in serum-free media containing 33 μM bovine serum albumin (BSA) for 6 hours. Cells and media were harvested; cells were assayed for total protein and media was assayed for acid soluble material (ASM), an indicator of FAO [Methods]. Results are expressed as ASM, nmoles/mg protein and represented as the average ± range of duplicate samples.

Figure 5S. Regulation of PDK4, ATGL and Rictor mRNA by fatty acids, PPAR agonist and antagonist in HepG2 cells. Panels A & B. HepG2 cells were treated with EPA (100 μM), GW0742 (1 μM) [Panels A & B] or cis-VA (100 μM) [Panel C) in serum free media containing 33 μM BSA for the times indicated in the figure. RNA was extracted and PDK4, ATGL, rictor and cyclophilin mRNA was quantified by qRT-PCR. Results are expressed as mRNA abundance-Fold Change for PDK4 (Panel A), ATGL (Panel B); and Rictor (Panel C); mean ± SD, n=3. Panel D. HepG2 cells were treated with vehicle (Veh) or cis-VA (100 μM) with BSA as above in the absence or presence of PPAR subtype specific antagonist GW6471 (PPARα, 1 μM), GSK3787 (PPARβ, 1 μM) or T0070907 (PPARγ, 4 nM) for 48 hrs. ATGL and cyclophilin RNA was quantified as

above and represented as the mean ± S.D., n=6. *a*, $p<0.05$ versus vehicle-treated cells. Student's t-test.

Supplemental Fig. 1S

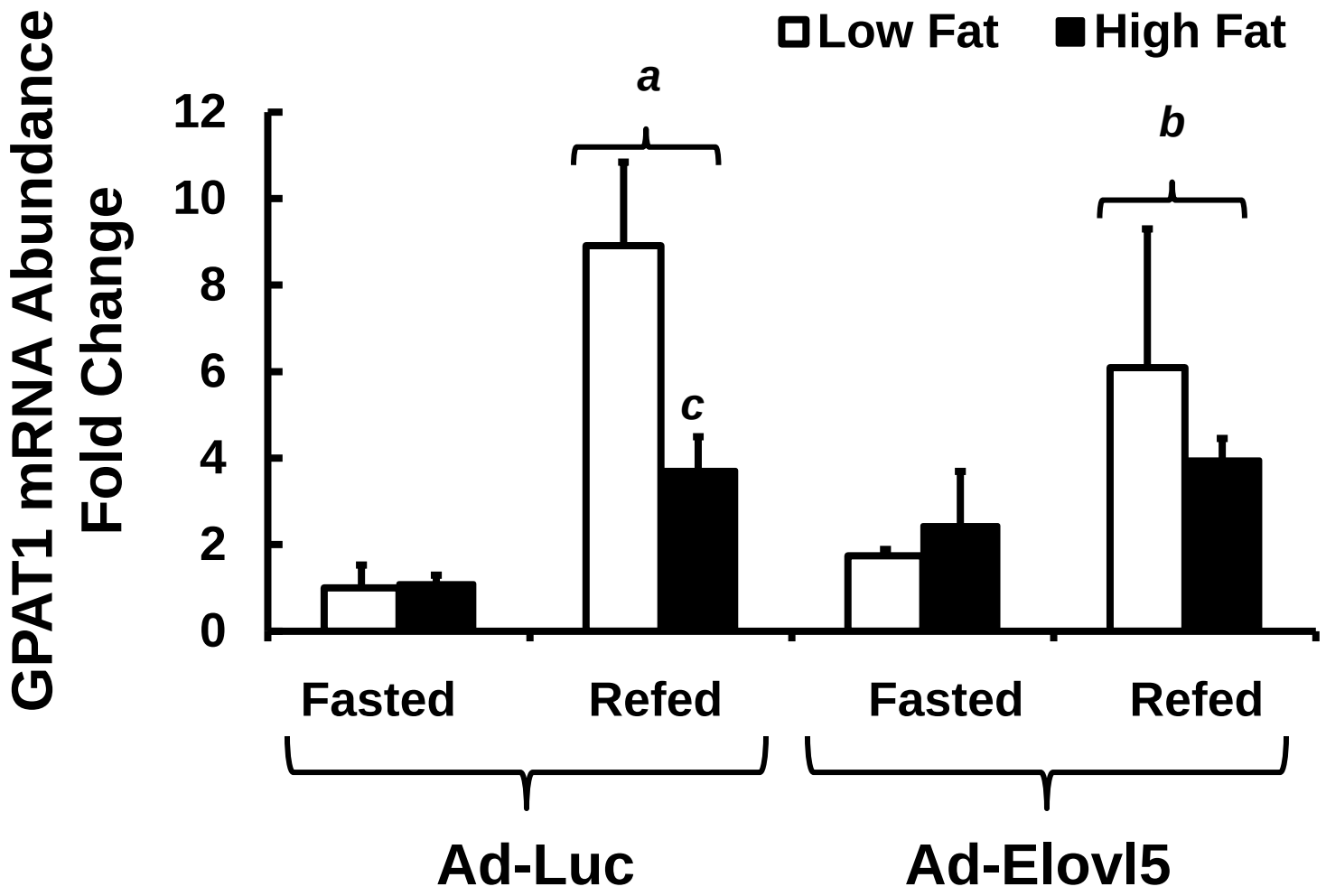

Supplemental Fig. 2S

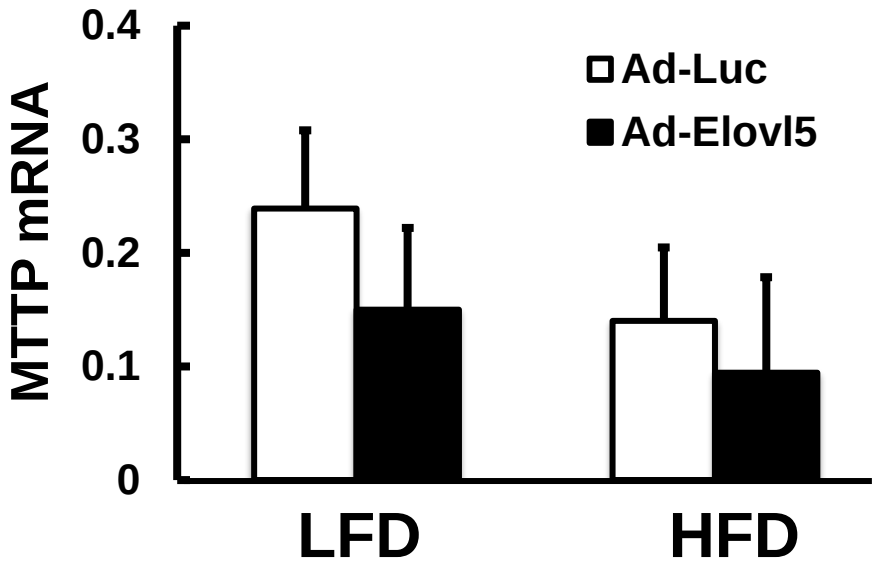

Supplemental Fig. 3S

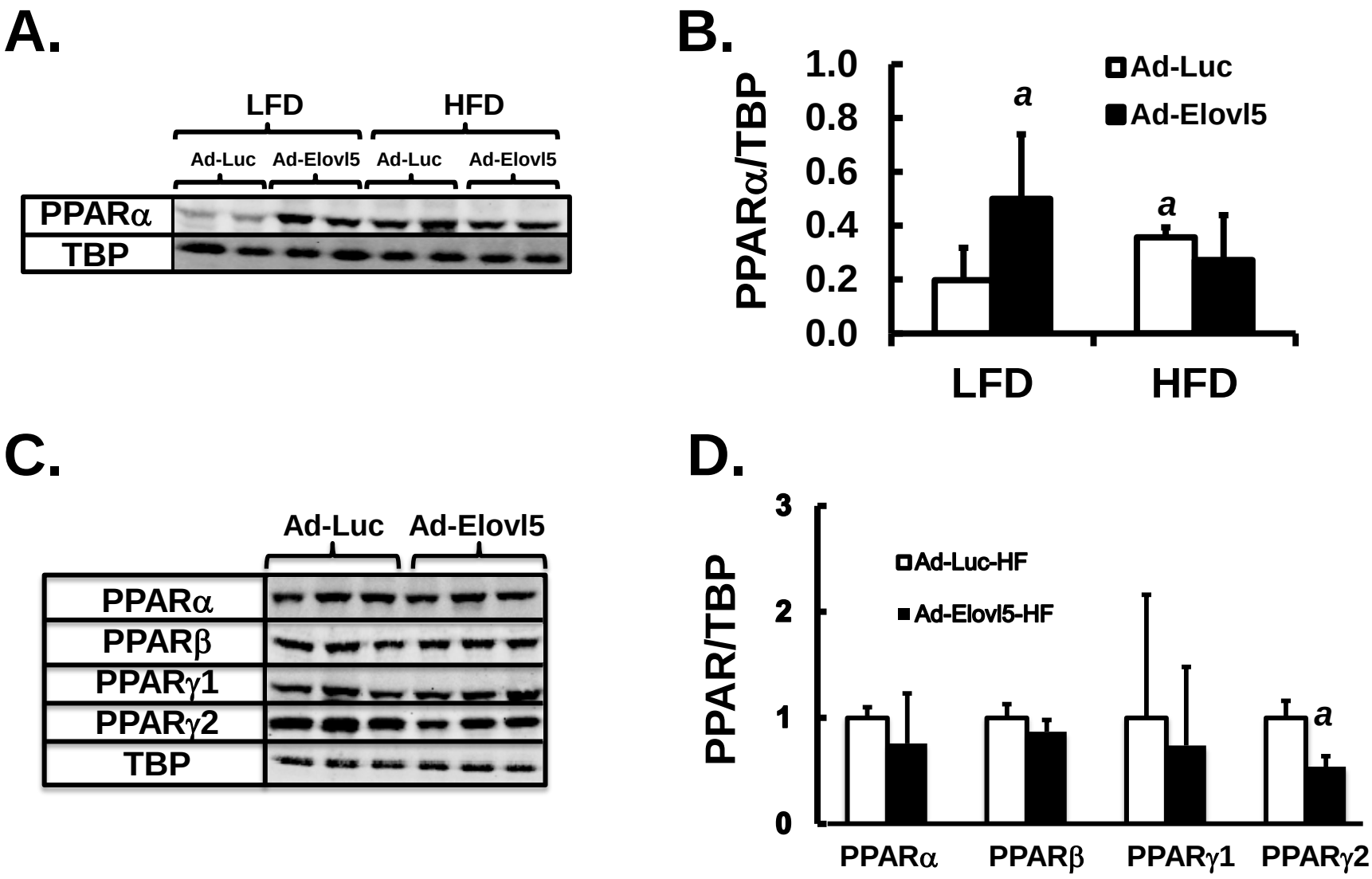

Supplemental Fig. 4S

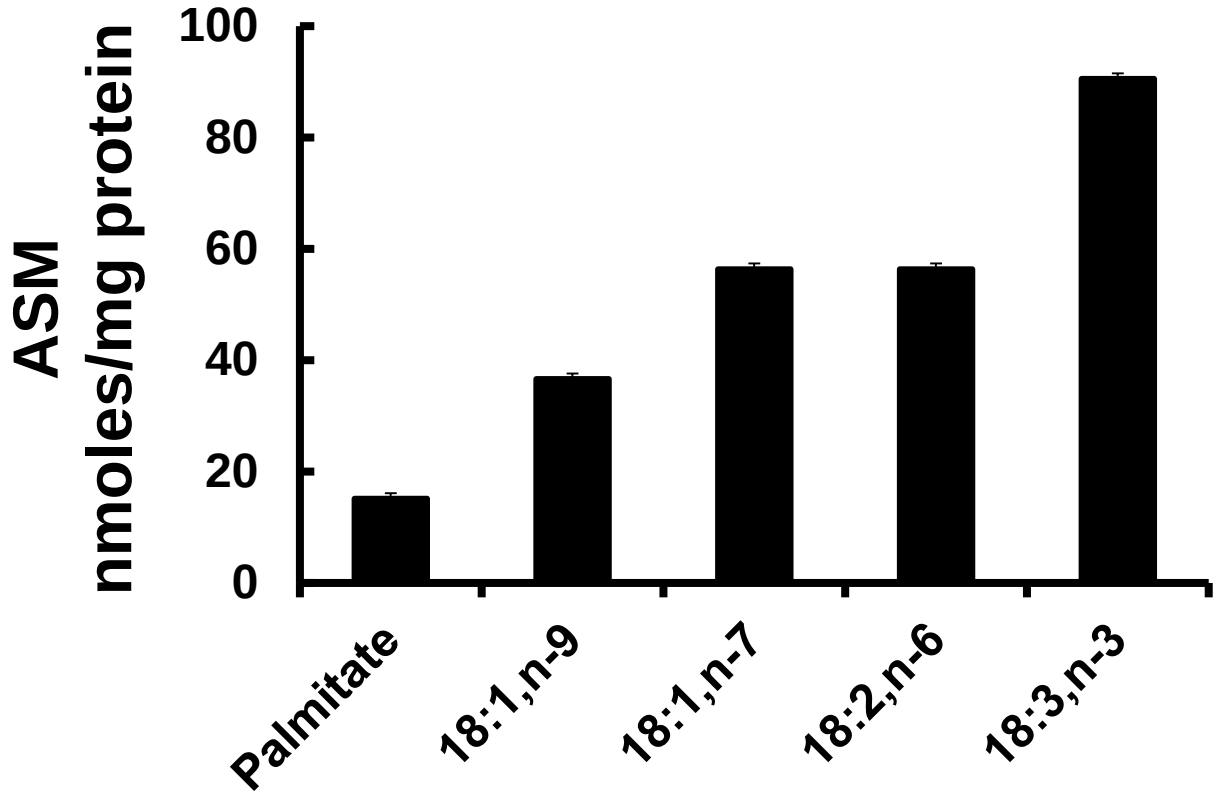

Supplemental Figure 5S: